St Petersburg University
www.spbu.ru

RUSSIAN FOUNDATION FOR BASIC RESEARCH
RFBR

Field electron emission spectroscopy of silicon carbide

Konstantin Nikiforov[1*], Vasiliy Trofimov[1], **Nikolay Egorov**[1**]
Vladimir Ilyin[2], Vladimir Golubkov[2], Alexey Ivanov[2]

[1]Saint Petersburg State University, St. Petersburg, Russia
[*]k.nikiforov@spbu.ru [**]n.v.egorov@spbu.ru
[2]Saint Petersburg Electrotechnical University "LETI", St. Petersburg, Russia

Invited Presentation at
7th ITG International Vacuum Electronics Workshop (IVEW) and 13th International Vacuum Electron Sources Conference (IVeSC), May 26-29, 2020, Bad Honnef

OUTLINE

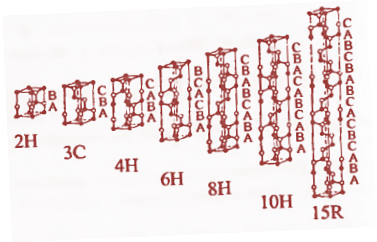

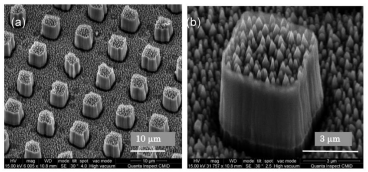

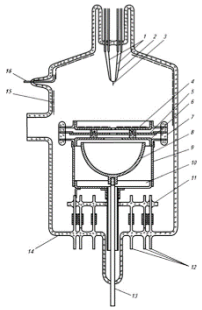

- Introduction to silicon carbide materials and history
- SiC FEAs
- Field emission spectroscopy method
- Measurement setup
- Field electron emission spectroscopy of SiC
- Results of experiment
- Discussion and Conclusion

SILICON CARBIDE: SIC POLYTYPES

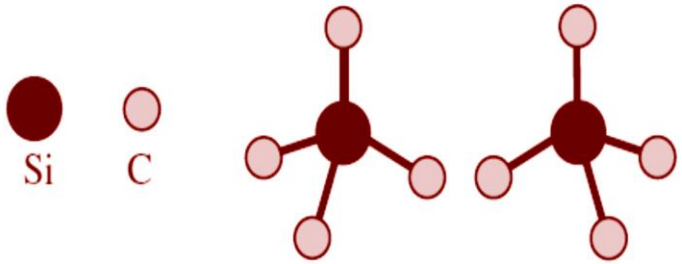

Two types of tetrahedrons forming the building blocks of all SiC crystals with each tetrahedron consisting of one Si atom and four covalently bonded nearest-neighboring C atoms. One type is obtained by rotating another type around its c-axis (vertical here) by 180° (Fan et al. 2014).

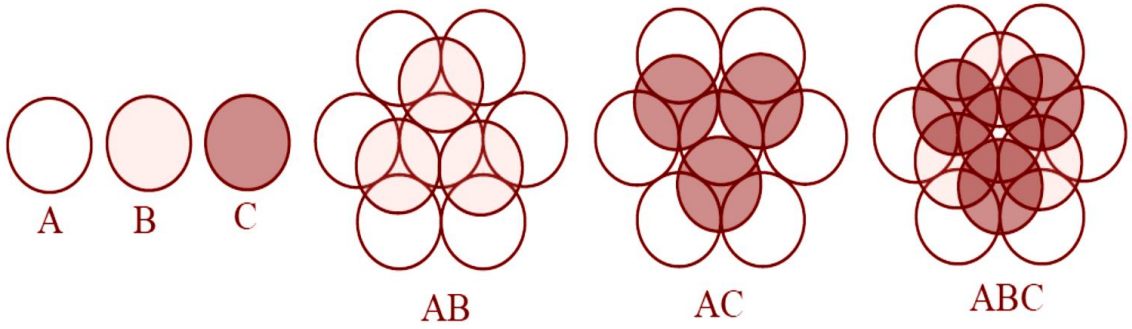

Three types (A, B, C) of Si–C double-atomic layer arrangement along the c-axis (stacking direction) through close-packed spheres. The c-axis is normal to the paper plane (Fan et al. 2014).

SILICON CARBIDE: SIC POLYTYPES

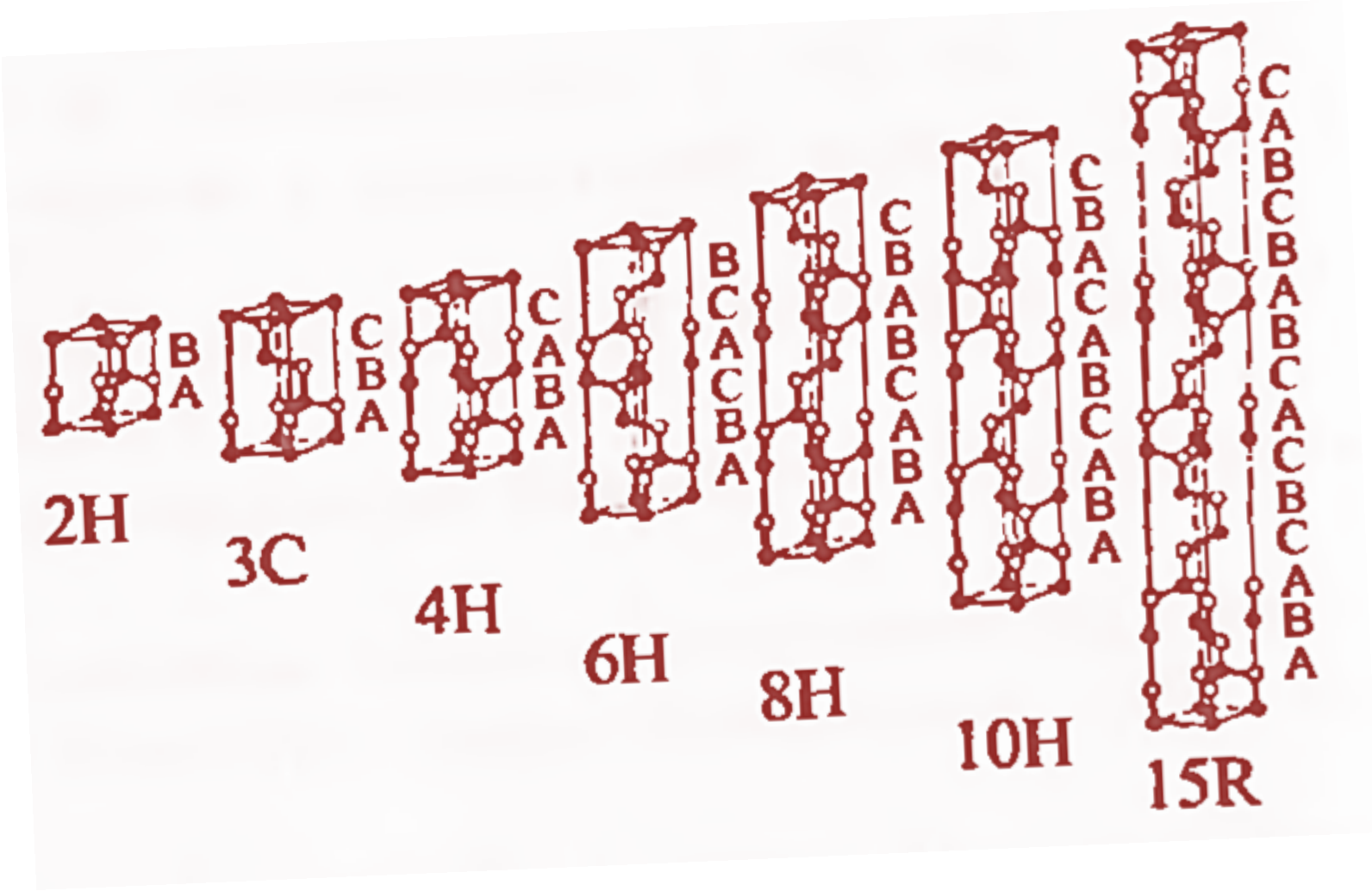

COMPARISON OF MATERIALS PROPERTIES

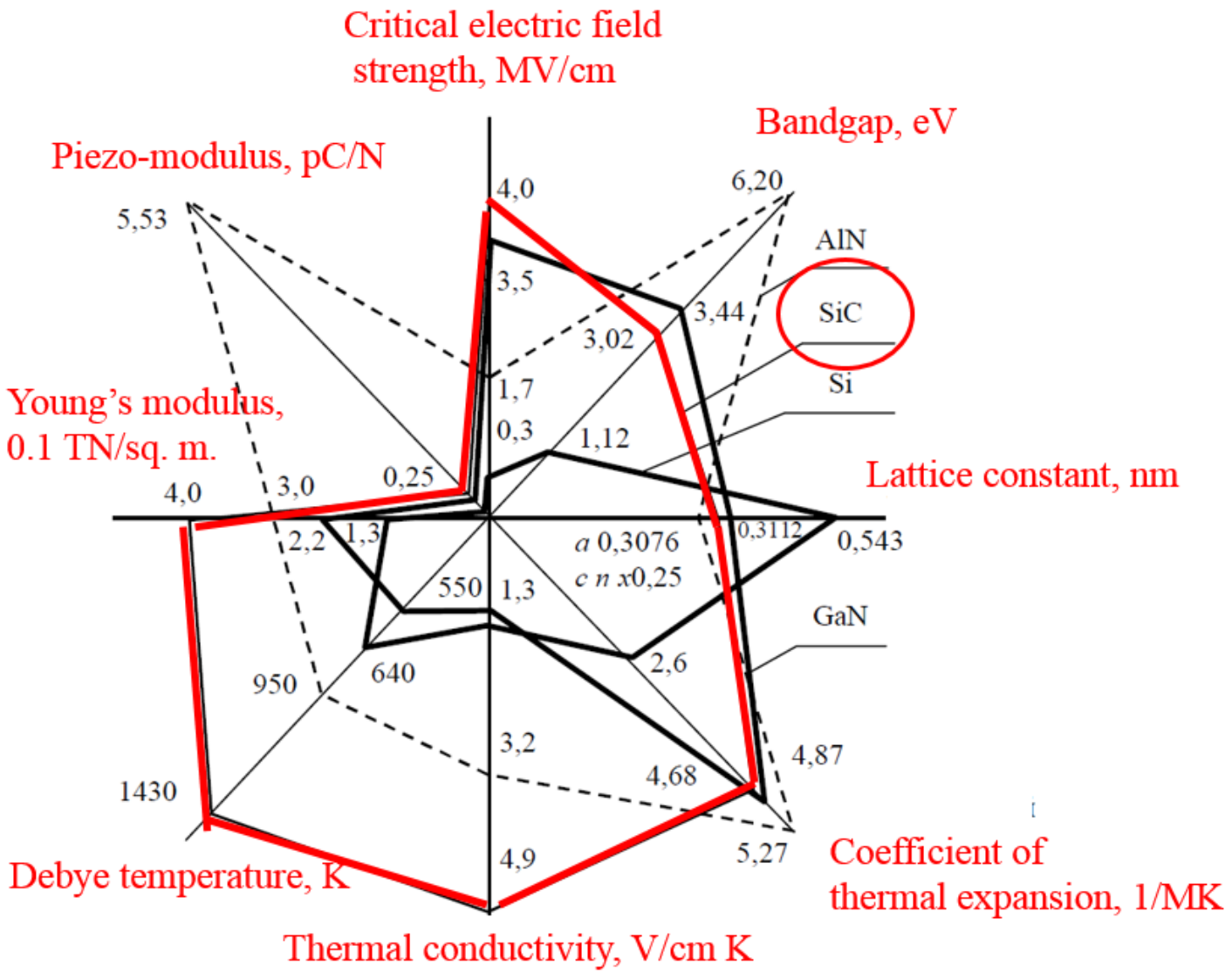

SIC FIELD EMISSION ARRAY TECHNOLOGY

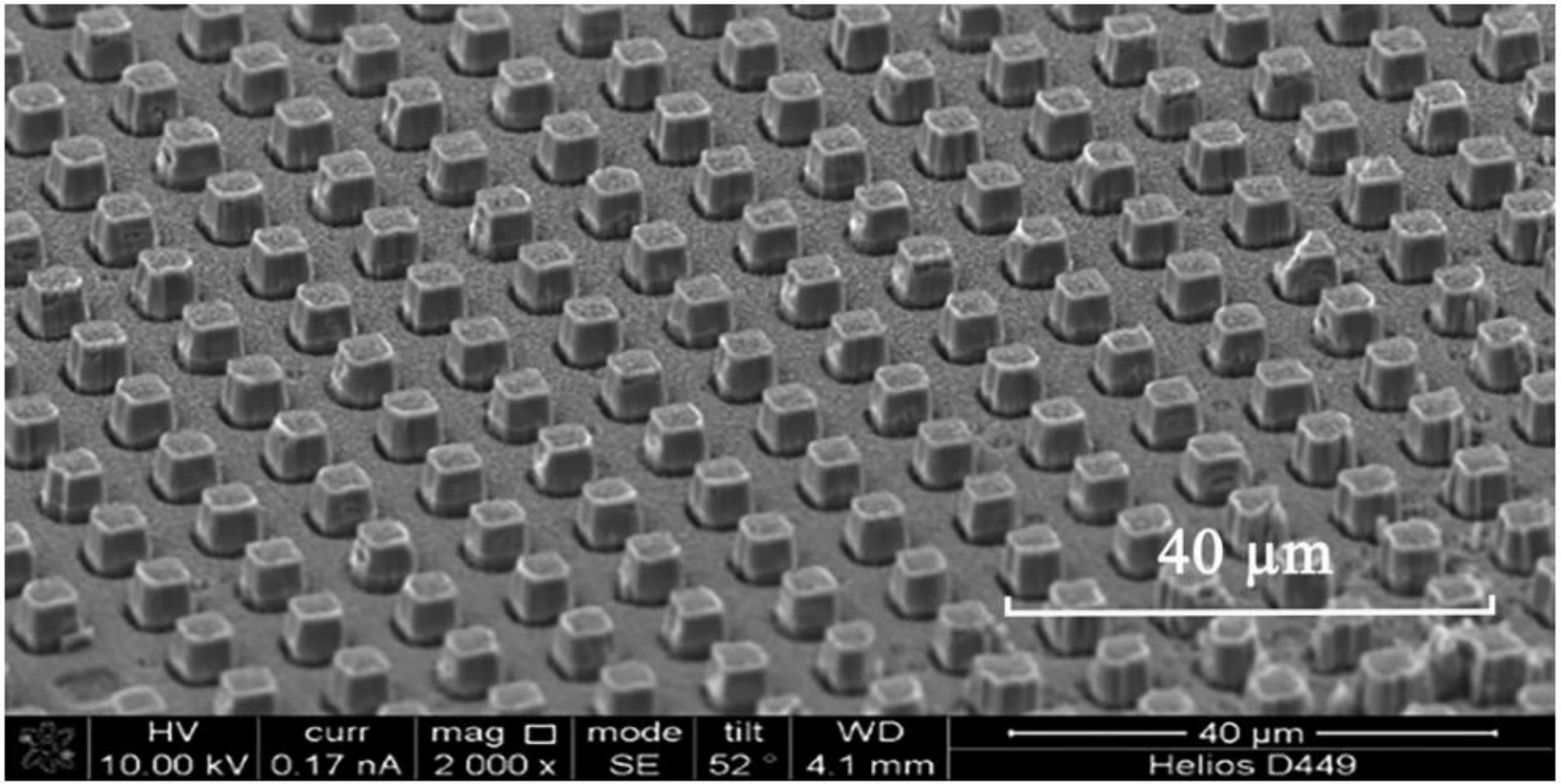

SEM micrograph of the silicon carbide field emission array with a period of 10 µm. A single pedestal has a height of 8.5 µm and a crosssectional area of 5 x 5 sq. µm (Golubkov et al. 2016).

SIC FIELD EMISSION ARRAY TECHNOLOGY

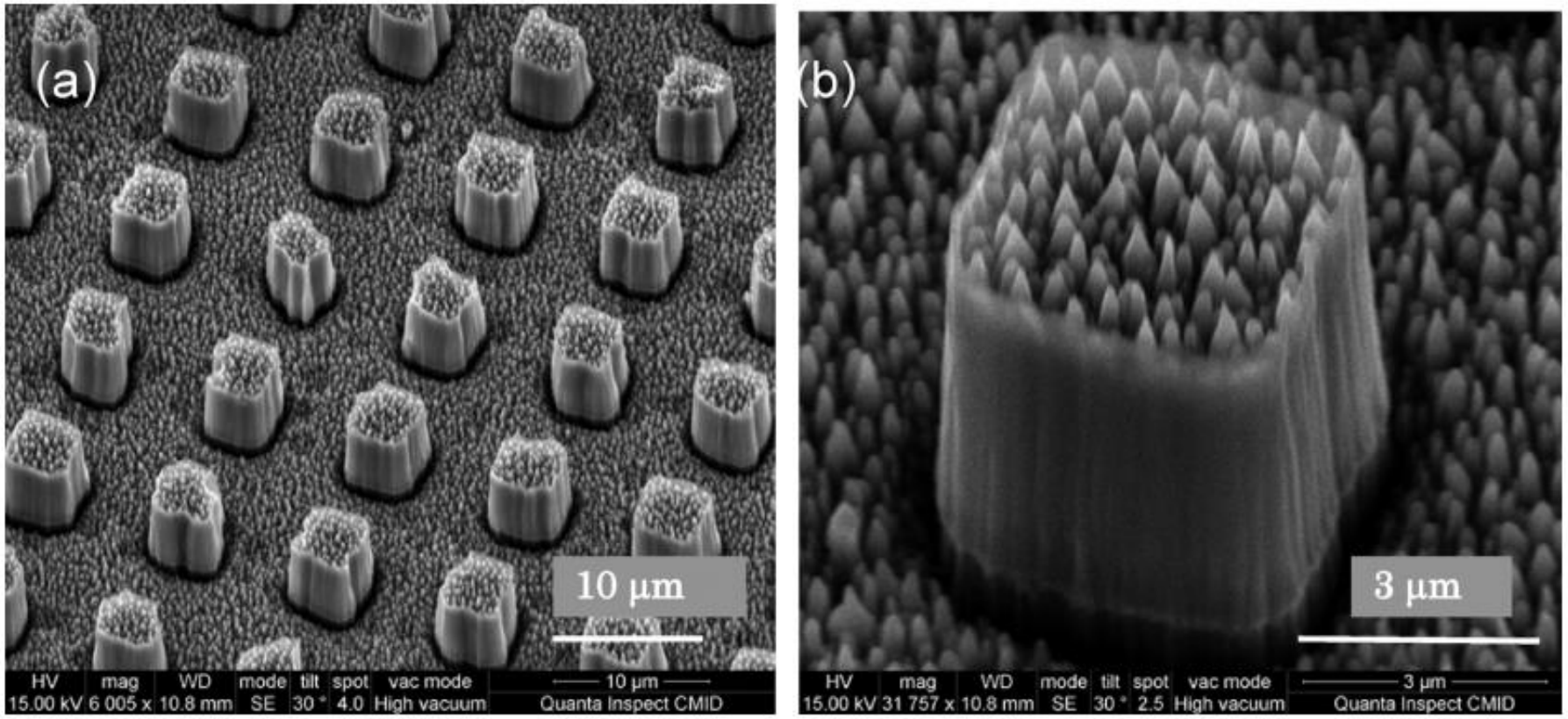

SEM micrographs of (a) 6H-SiC array of pedestals and (b) 6H-SiC pedestal with nanoscale tips. The dimensions of a single tip are as follows: radius: 30 nm, height: 2 µm, and base diameter: 0.3 µm (Golubkov et al. 2016).

OPTIMIZATION OF STRUCTURE AND FEF

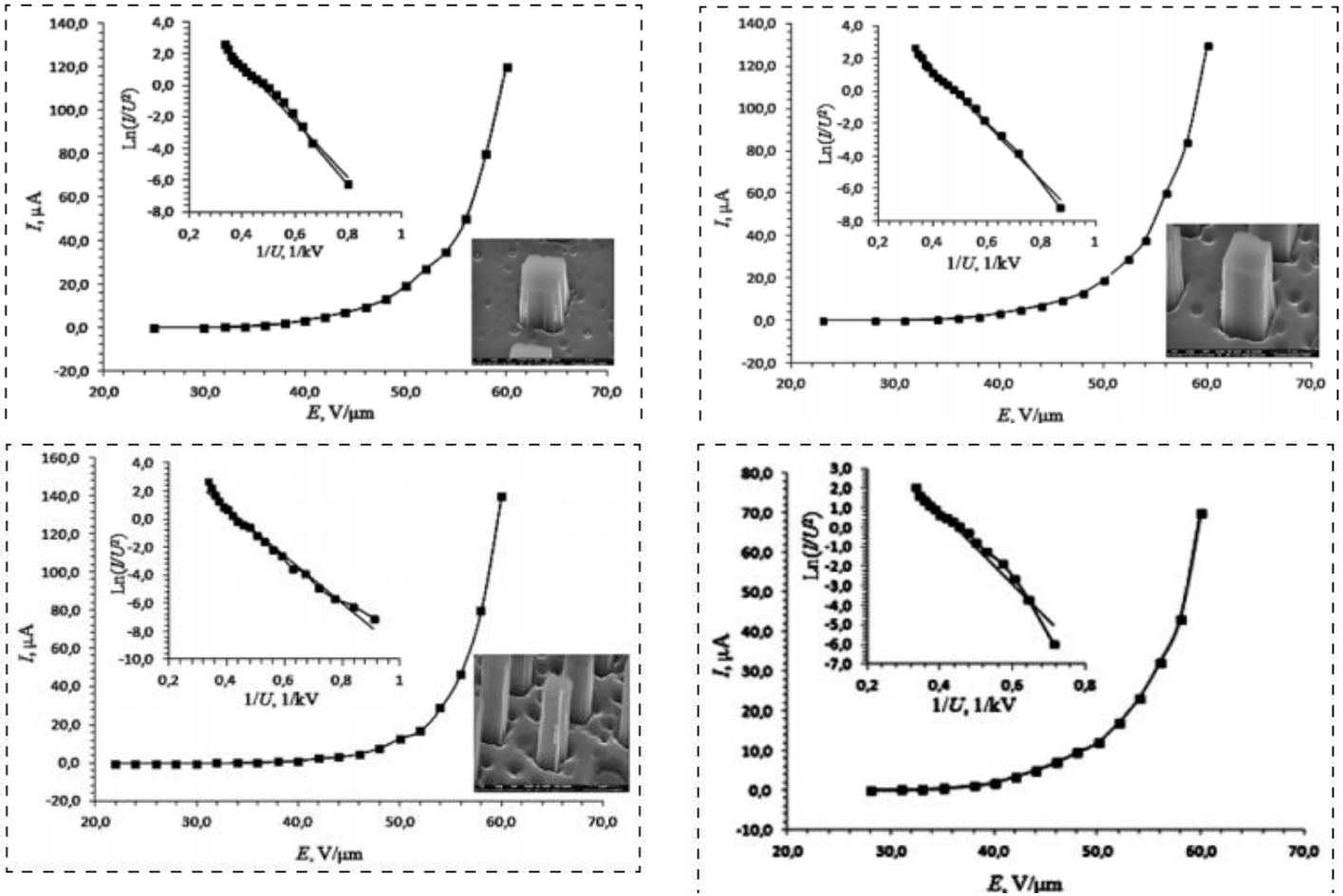

CVC of the sample with a height of pedestals of 6, 12, 18, 3 μm. Insets: left — CVC in the coordinates of Fowler—Nordheim; right — SEM image of the pedestals μm (Afanasiev et al. 2015).

SILICON CARBIDE: BLADES VS. TIPS

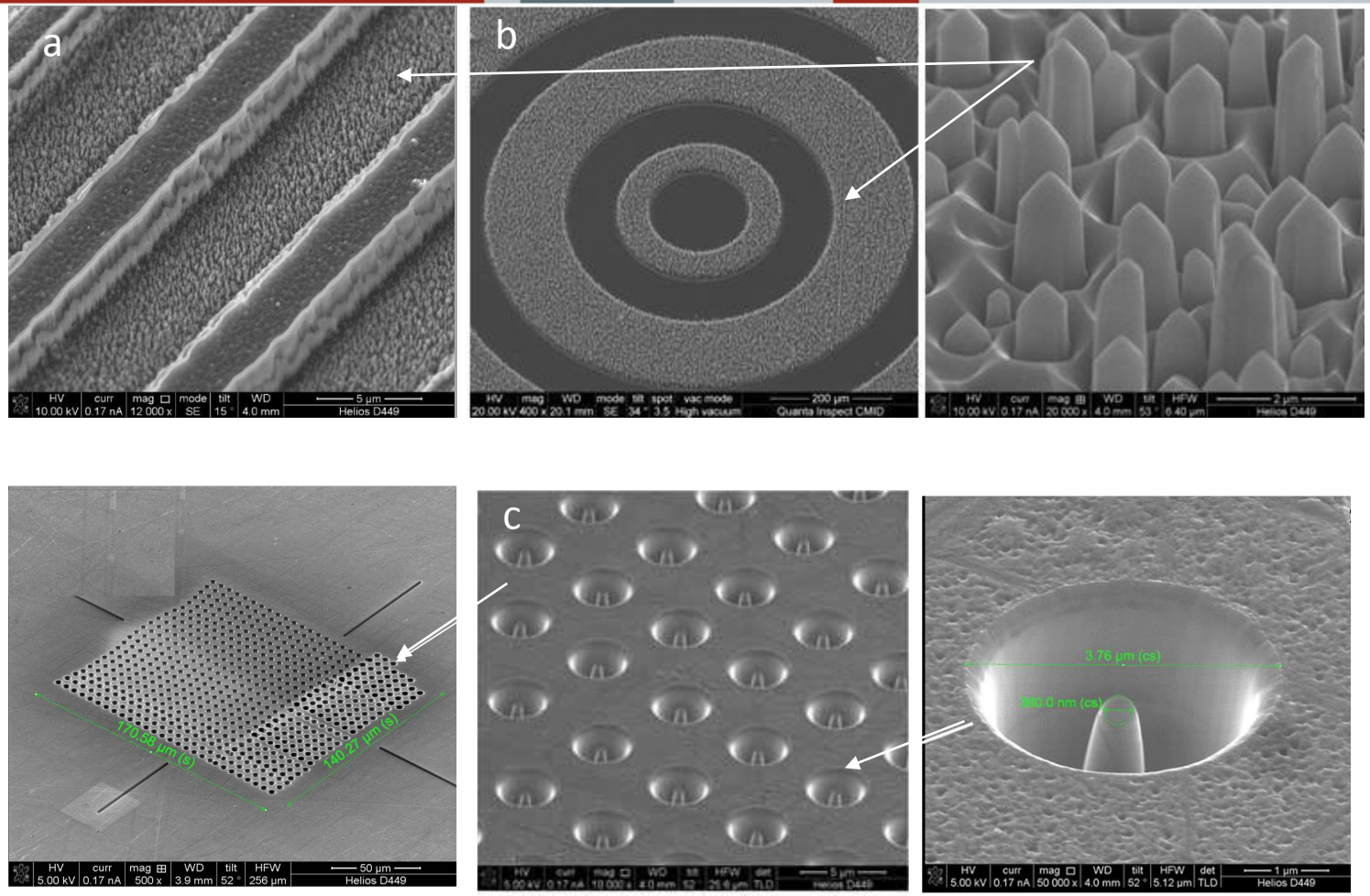

a) SEM image of linear blade triode structure (Afanasyev et al. 2018); b) SEM image of cylindrical blade structure (Afanasyev et al. 2017); c) FE array with cone-shape emitters (Kuznetsova et al. 2012).

FIELD EMISSION MICROSCOPES

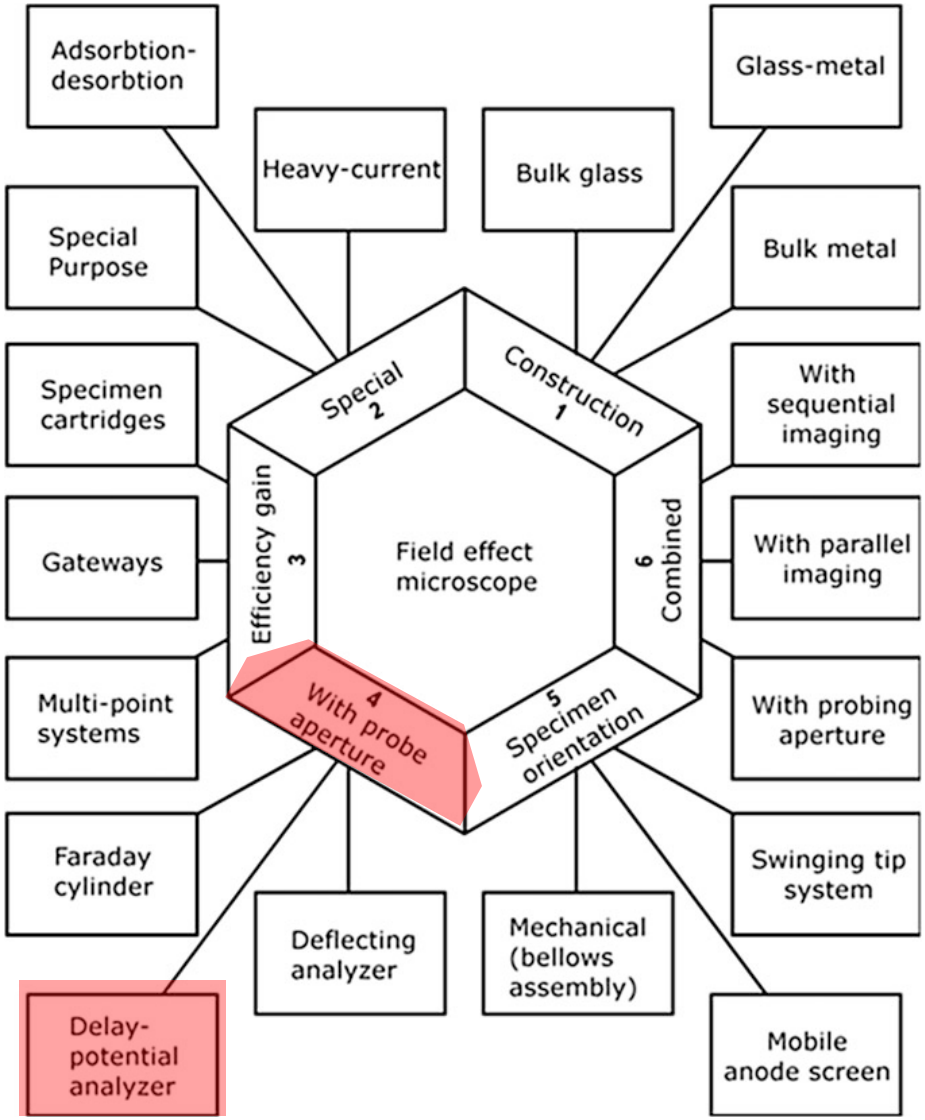

FIELD EMISSION ENERGY ANALYZER

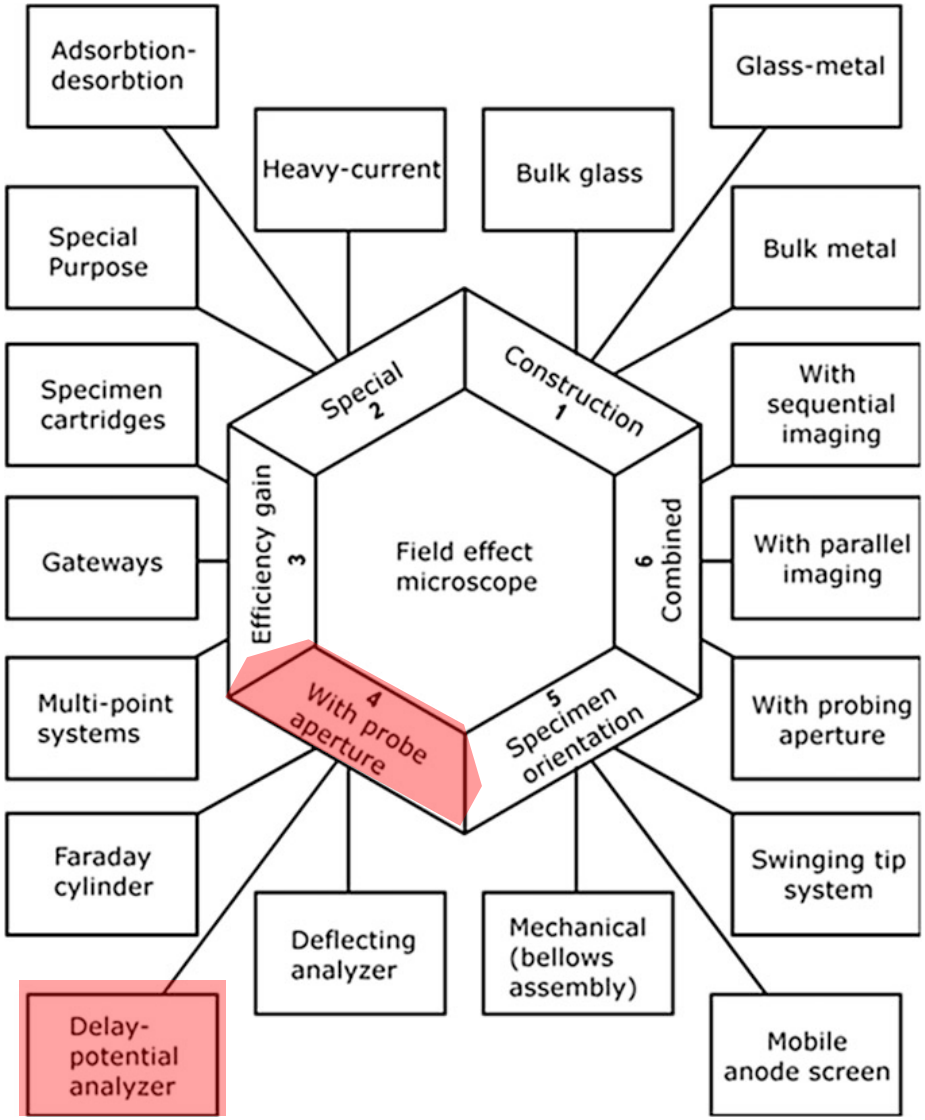

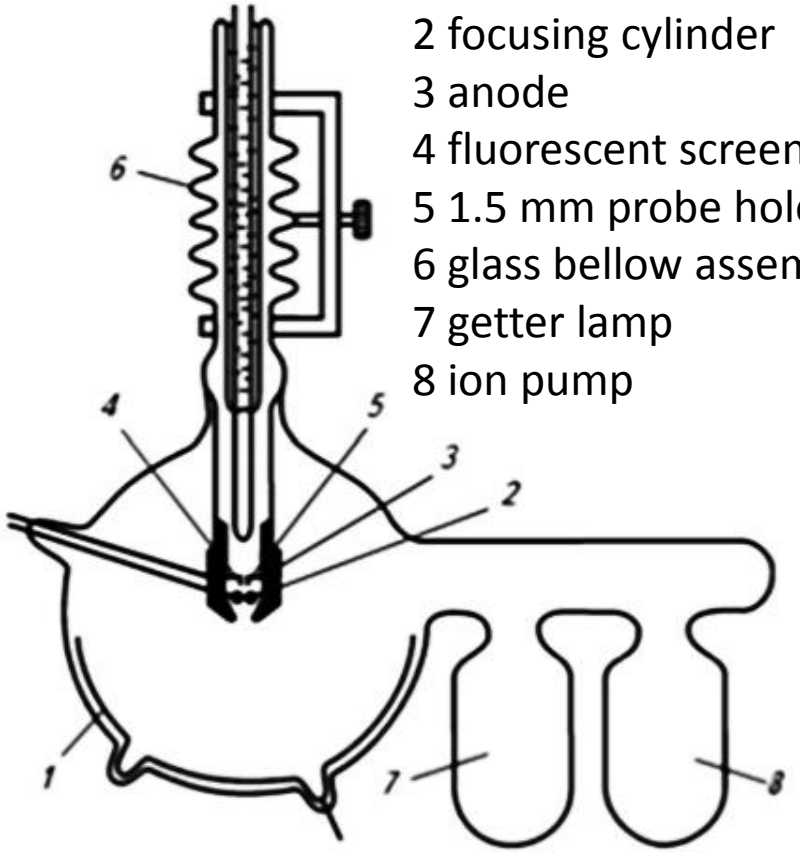

1 collector
2 focusing cylinder
3 anode
4 fluorescent screen
5 1.5 mm probe hole
6 glass bellow assembly
7 getter lamp
8 ion pump

Construction of the first design of energy analyzer with a retarding potential (Young and Mueller, 1959).

POTENTIAL DIAGRAM

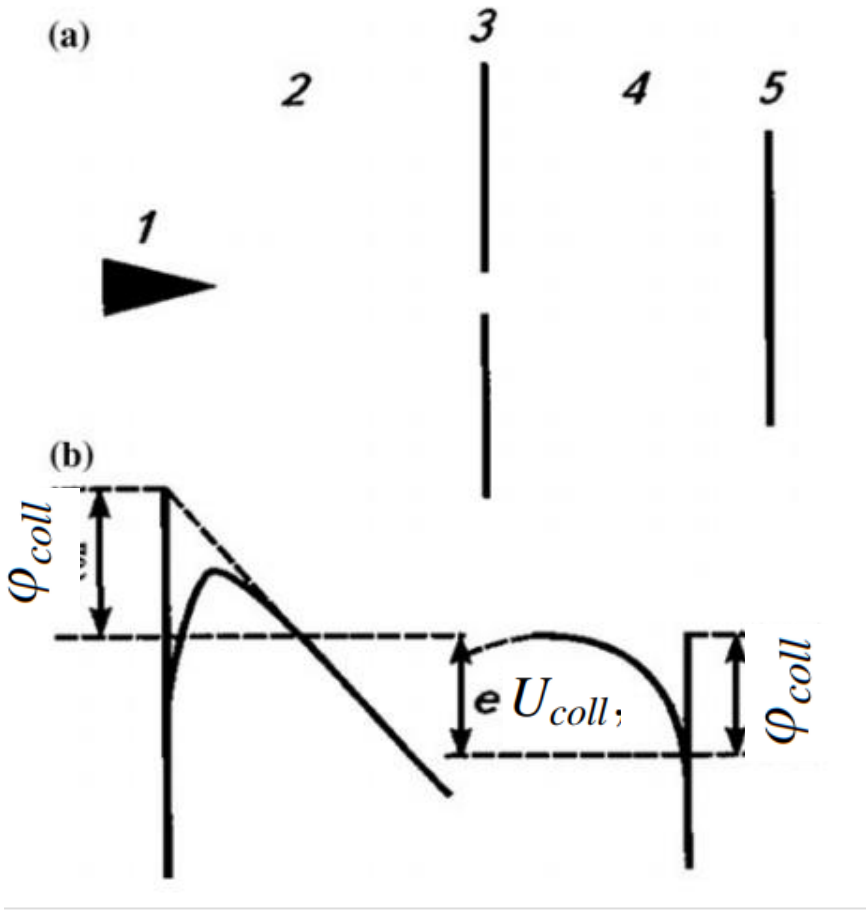

$$E > \varphi_{coll} + E_F - U_{coll},$$

$$I_{coll} = \int_{\varphi_{coll} - \varphi + U_{coll}}^{\infty} P(E)dE,$$

$$dI/dU_{coll} = P(\varphi_{coll} - \varphi + U_{coll}),$$

a) Scheme of a field electron energy analyzer with a retarding potential: (1) cathode, (2) acceleration area, (3) anode with a diaphragm, (4) retarding area, (5) collector.
b) Potential diagram of the analyzer.

RETARDING POTENTIAL ANALYZER

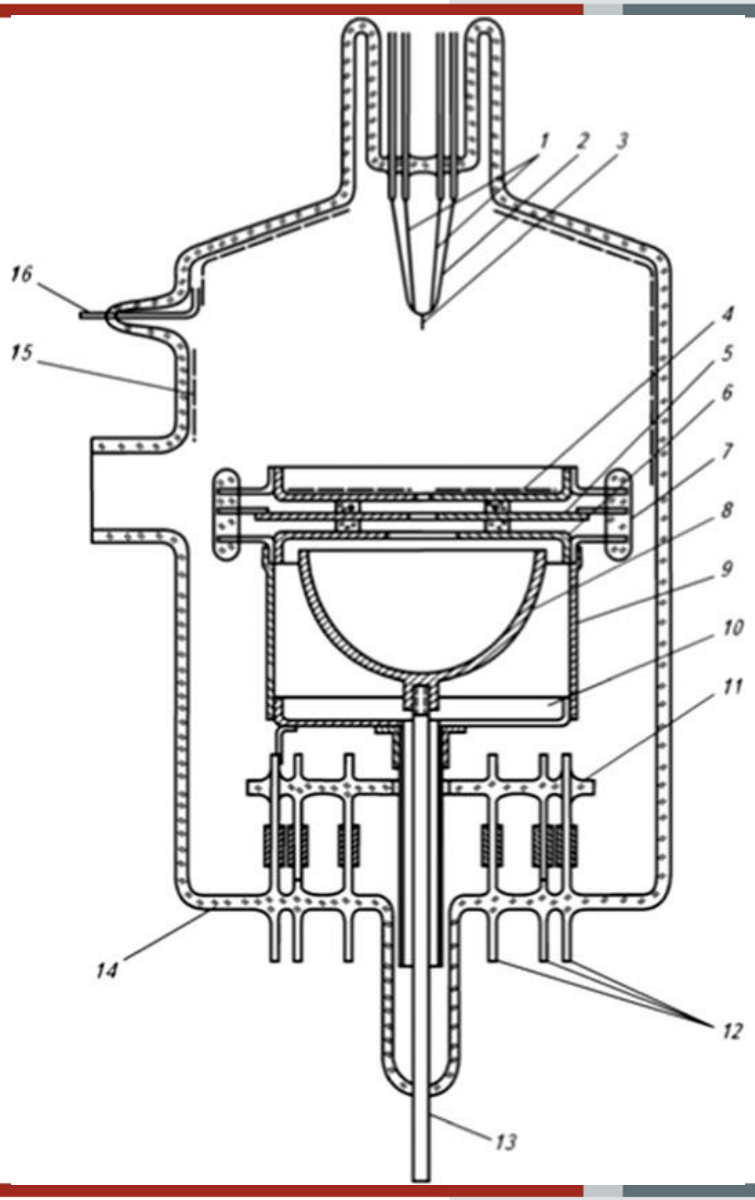

Construction of an analyzer with retarding potential and hemispherical collector:
1 measuring wires;
2 arch;
3 emitter;
4 anode cylinder with a probing hole;
5 focusing lens;
6 Faraday cylinder cover;
7 fixation «beads»;
8 hemispherical collector;
9 Faraday cylinder;
10 Faraday cylinder base;
11 mounting leg;
12 electrode lead-outs;
13 collector lead-out;
14 glass bulb;
15 conductive covering;
16 conductive covering lead-out
(Egorov and Sheshin, 2017)

ELECTRO-PHYSICAL SYSTEM OF ANALYZER

$$U = U_z + U_0 \sin \omega t$$

$$\frac{\mathrm{d}I_k}{\mathrm{d}U} \sim \frac{\mathrm{d}I_k}{\mathrm{d}\varepsilon} \sim \frac{\mathrm{d}N(\varepsilon)}{\mathrm{d}\varepsilon}$$

$$I_k = I_k(U_z + U_0 \sin \omega t)$$

$$I_k = I_k(U_z) + \left(\frac{\mathrm{d}I_k}{\mathrm{d}U}\right)\Big|_{U=U_z} U_0 \sin \omega t + \frac{1}{2!}\left(\frac{\mathrm{d}^2 I_k}{\mathrm{d}U^2}\right)\Big|_{U=U_z} U_0^2 \sin^2 \omega t + \ldots$$

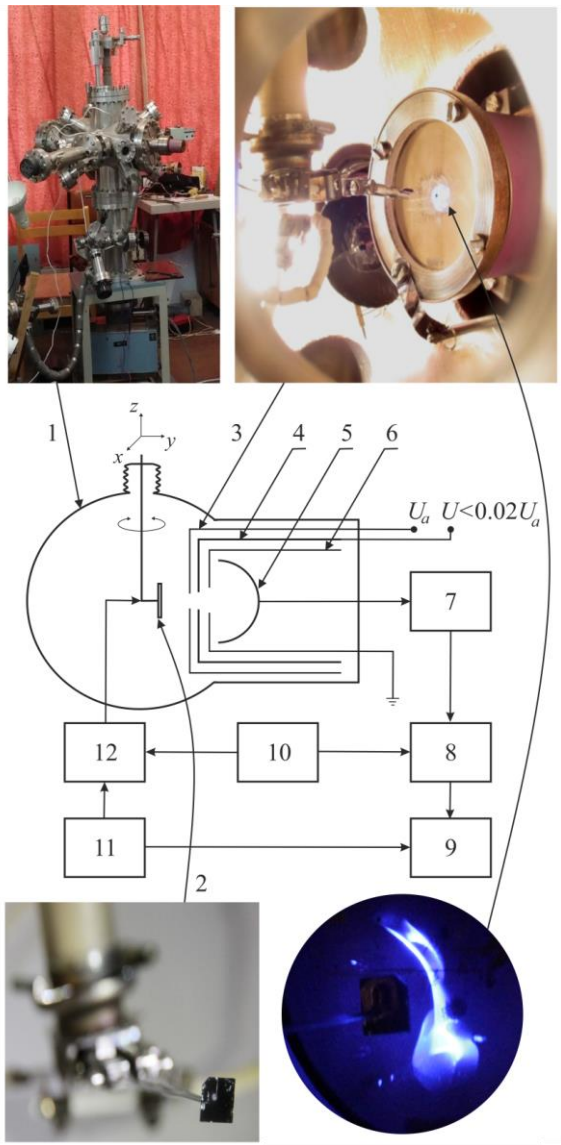

Construction of an analyzer with retarding potential and hemispherical collector: (7) electrometric amplifier; (8) synchronous detector; (9) registering device; (10) modulation block; (11) signal adder. Functional schematic of the experimental set up and FEA fixed in the sample fixation mechanism of the energy analyser with its emission image registered on a luminescent screen.

BOUNDARY FIELD ENHANCEMENT

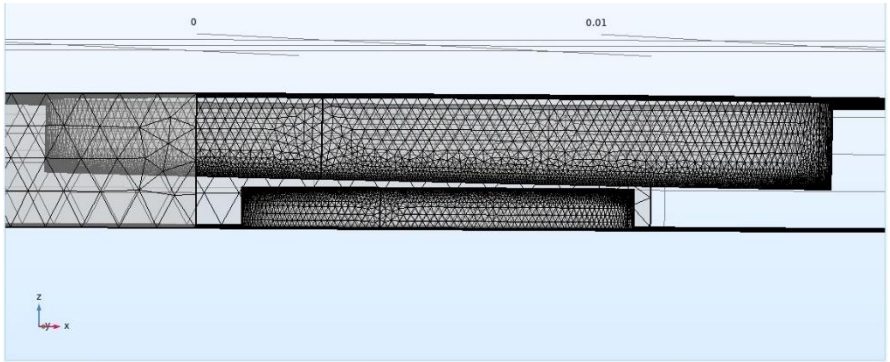

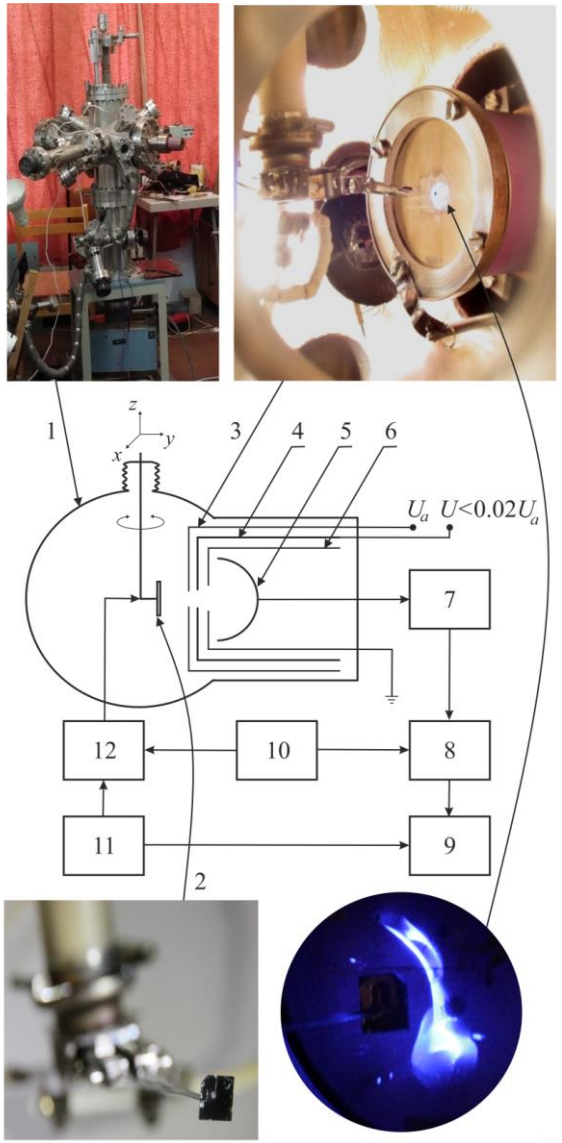

MICRODIODE FEA CONFIGURATION

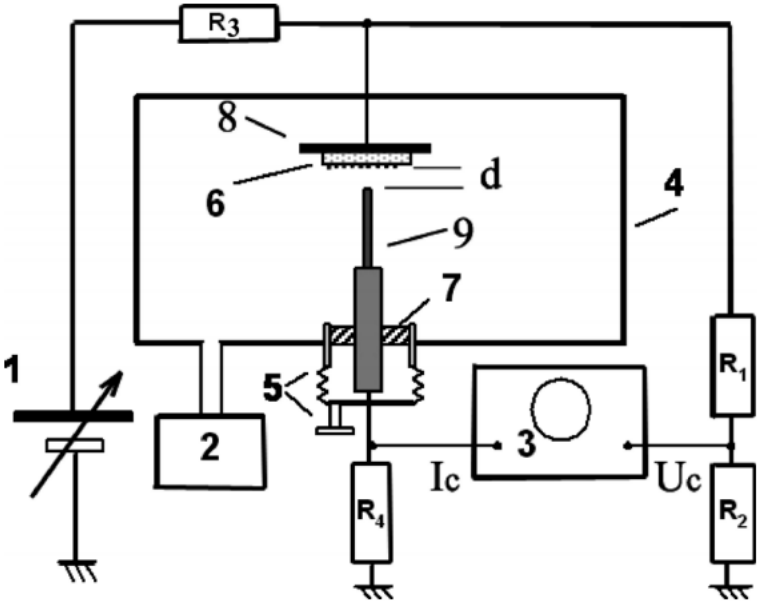

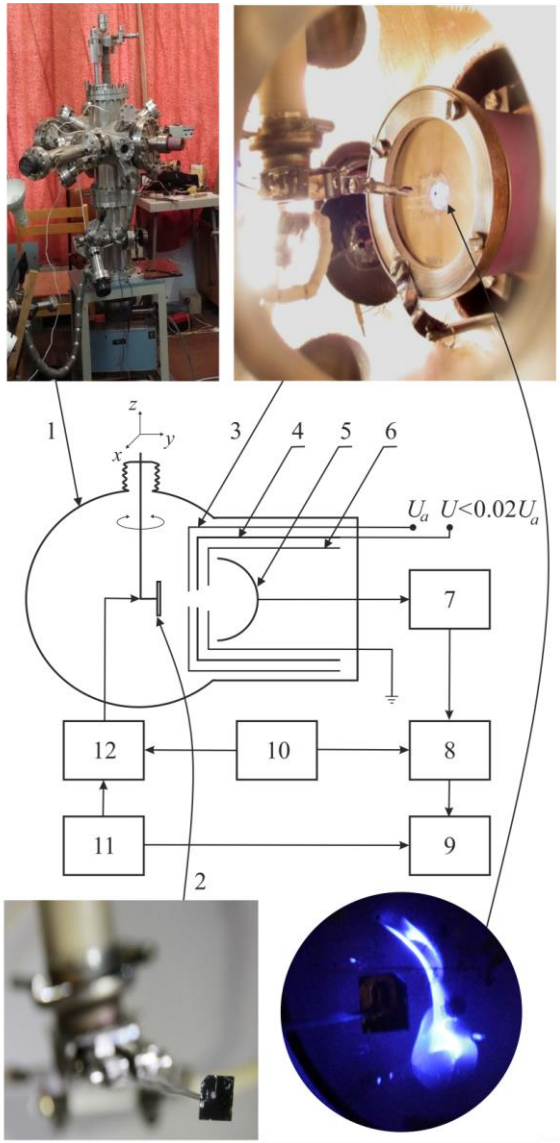

Experimental setup for microdiode configuration measurement: (1) DC high voltage generator, (2) vacuum pump, (3) oscilloscope TDS-3052B, (4) vacuum chamber, (5) anode position adjustment, (6) field emission array (cathode), (7) isolator, (8) cathode holder, and (9) movable anode, (R_1–R_4) inductively free resistors (Ivanov et al. 2018).

SIC MACROSAMPLE

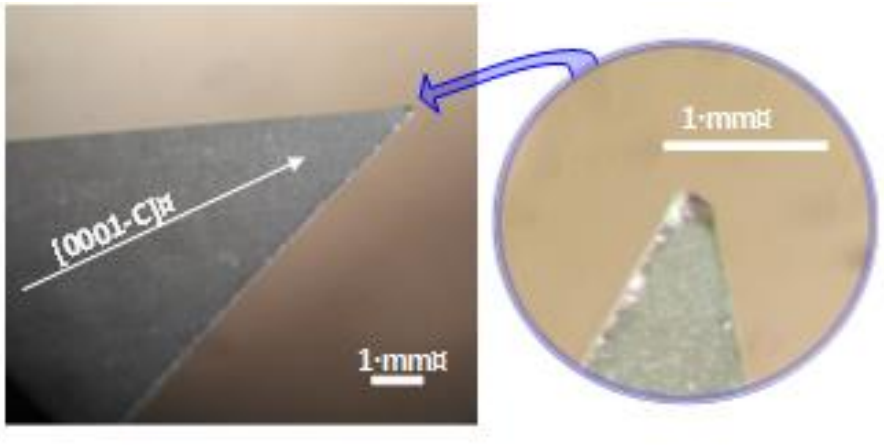

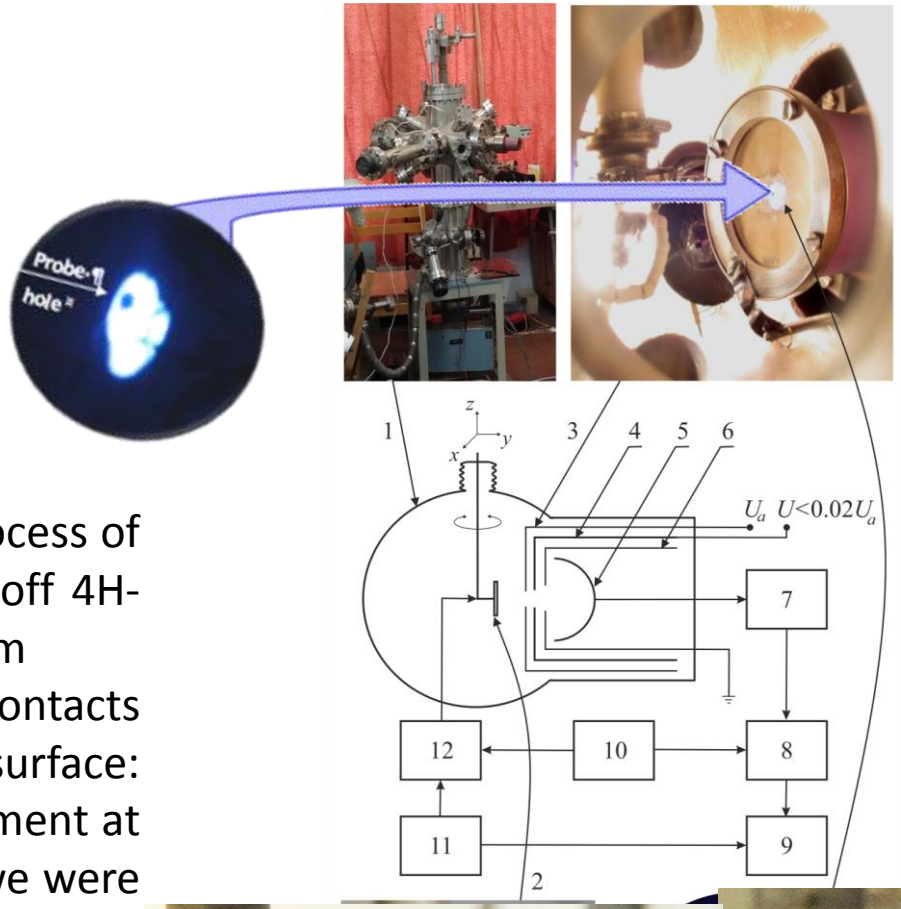

Optical microscope image of the SiC emitter.
Monocrystals of 4H-SiC doped by nitrogen in process of sublimation were grown in SPETU “LETI” at 4° off 4H-SiC wafers (0001-C). Resistivity ρ_v = 0.02 Ohm·cm (N concentration — 3·10^18 1/cm^3). Ohmic contacts were deposited on both sides of non-emission surface: Ni/Ti/SiC (Ti — 50 nm, Ni — 300 nm, heat treatment at 1000°C, 2 minutes in vacuum 10 Pa). Because we were interested in examining the specimens as they were made, the ends were not etched down up to fine points as is the normal practice.

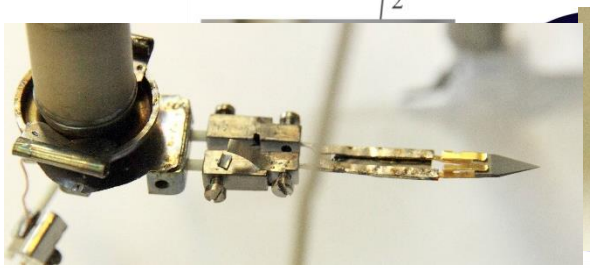

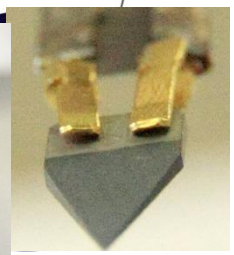

RESULTS OF EXPERIMENT

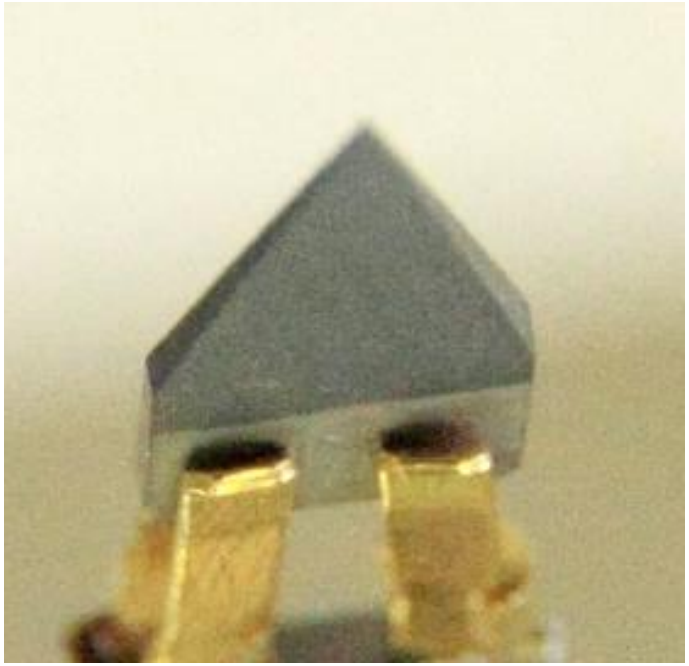

Specimen base in cross section — 0.1 by 0.6 cm.

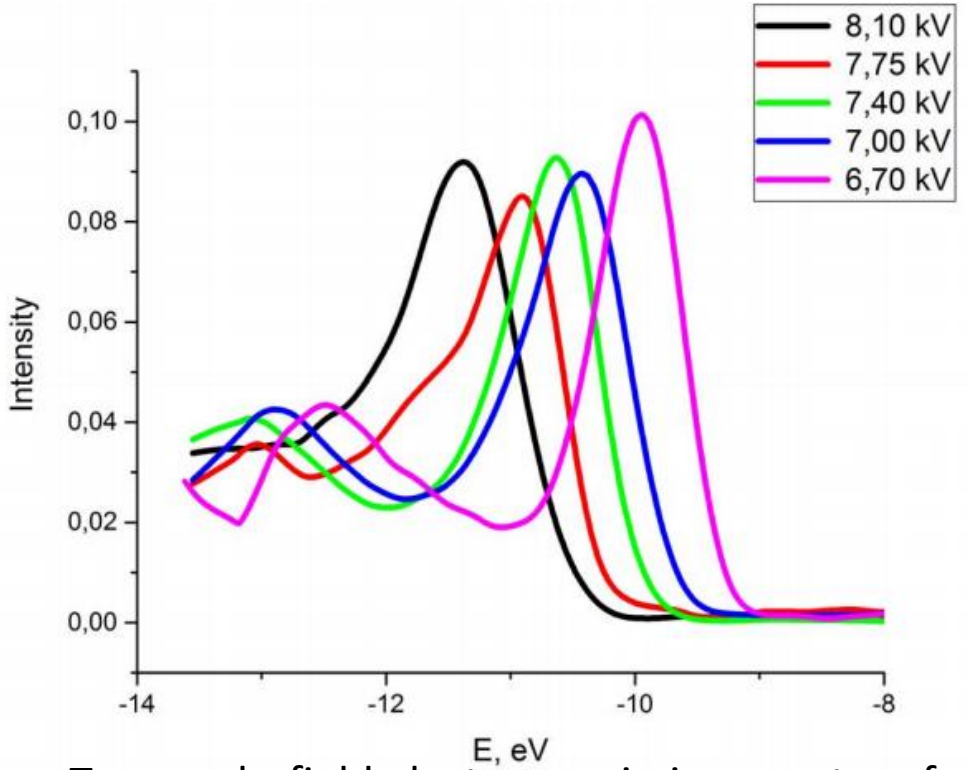

Two-peaks field electron emission spectra of of 4H-SiC:N (in a.u., normalized by integral counts) measured at bias voltages 6.7–8.1 kV.

The measured spectra reveal strong emission from conduction band (right peak) and weak emission from other states, the difference between two maxima is about 22% less than band gap of 4H-SiC (3.2 eV).

RETARDATION CURVE

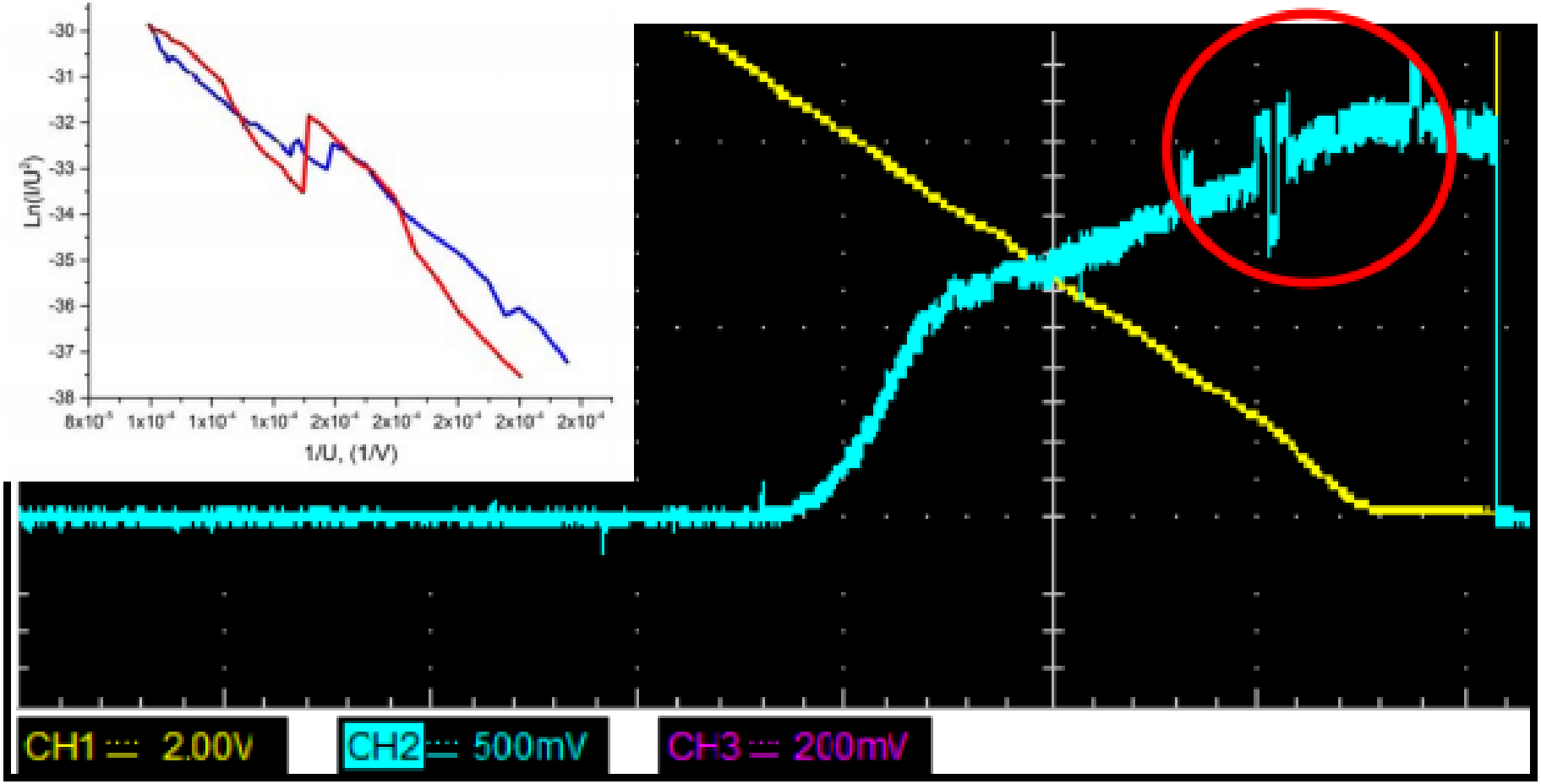

RESONANT TUNNELLING EFFECTS

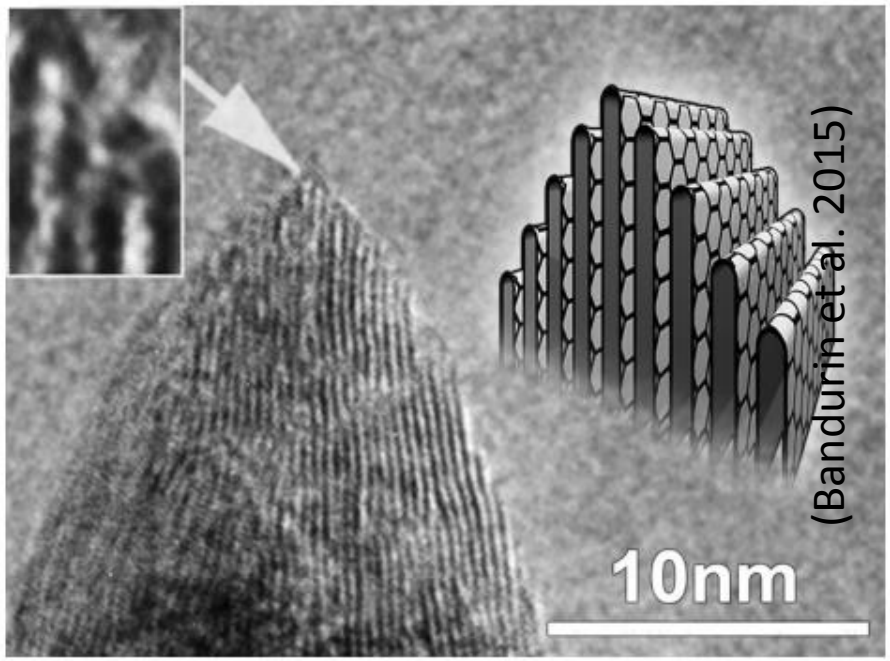

TEM image and scheme of a nanographite flake top edge showing its atomic arrangement with graphene layers connected in pairs. Inset shows enlarged image of atomic structure at top end of the nanographite flake.

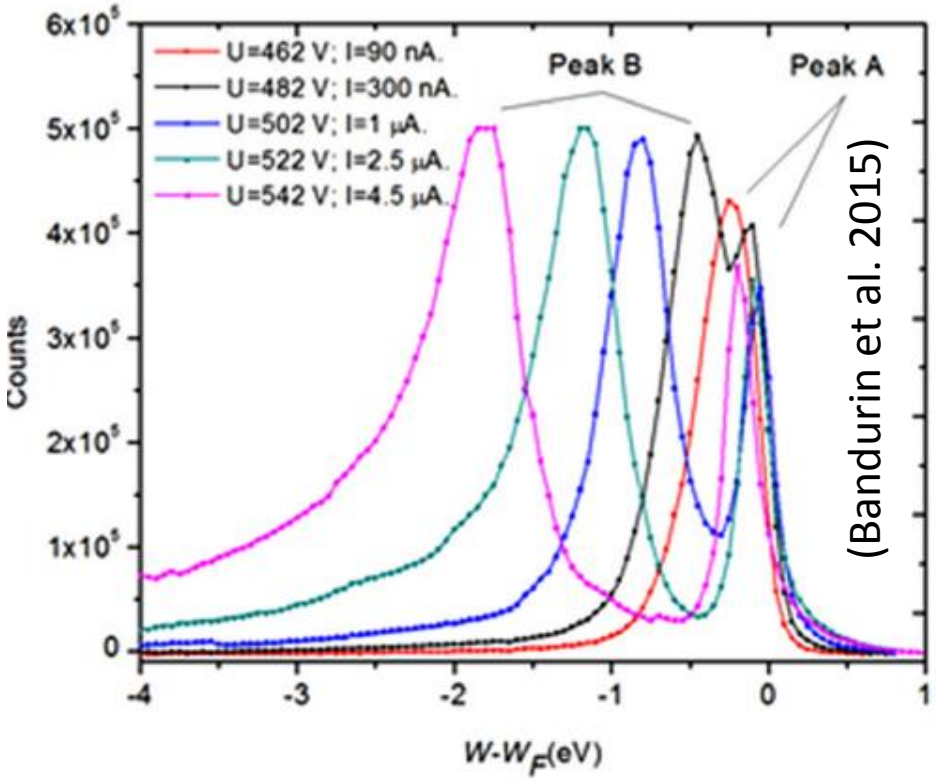

Two-peaks field electron emission spectra of a nanographite film measured for different values of emission current (Bandurin et al. 2015).

CONCLUSION

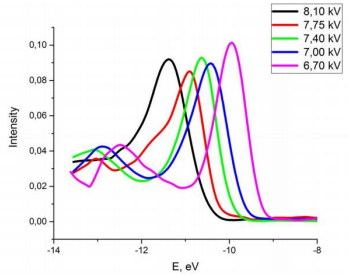

- The principal result is the study of the emitted electron spectra from silicon carbide in total energy distributions measurements by the retarding potential method.
- A peculiar feature, revealed from the FEED patterns is the existence of two maxima.
- The shape of the energy spectra suggests that electron emission is strong from conduction band and weak from an area below the conduction band.

REFERENCES

Afanasiev, A.V., Golubkov, V.A., Ilyin, V.A., Luchinin, V.V., Pronin V.P., and Serkov, A.V. **(2015)** "Array Field Emission Cathodes Based on Silicon Carbide with a Nanostructured Surface", *Nano- and microsystems technology*, 12, 49-55.

Afanasyev, A.V., Golubkov, V.A., Ivanov, A.S., Ivanov, B.V., Ilyin, V.A., Korlyakov, A.V., Lagosh, A.V. **(2017)** "Family of Silicon Carbide Solid State, Vacuum and Micromechanical Switches for Harsh Environments", *Microwave Electronics and Microelectronics,* 1(1) 80-84 (in Russian, Proceedings of VI Pan-Russian conference, St. Petersburg, SPETU "LETI", May 29-June 1 2017)

Afanasyev, A.V., Golubkov, V.A., Ivanov, A.S., Ilyin, V.A., Luchinin, V.V., Kurtash, V.A., and Serkov, V. **(2018)** "Investigation of a Possibility of Development of a Triode Type Electron Field Source Based on 4H-SiC-Structure with a Semi-Insulating Epitaxial Layer", *Nano and Microsystems Technology*, 20, 719-726 doi: 10.17587/nmst.20.719-726 (in Russian, Nano- i Mikrosistemnaya Tehnika)

Bandurin, D.A., Mingels, S., Kleshch, V.I., Lutzenkirchen-Hecht, D., Muller, G., and Obraztsov A.N. **(2015)** "Field emission spectroscopy evidence for dual-barrier electron tunnelling in nanographite", *Appl. Phys. Lett.* 106, 233112.

Egorov, N., and Sheshin, E. **(2017)**Field emission electronics. Springer.

Fan, J., and Chu, P. K. **(2014)** Silicon Carbide Nanostructures: Fabrication, Structure, and Properties. Springer.

REFERENCES

Golubkov, V.A., Ivanov, A.S., Ilyin V.A., and Luchinin, V.V. **(2016)** "Stabilizing effect of diamond thin film on nanostructured silicon carbide field emission array", *JVST B*, 34(6), 062202.

Ivanov, O.A., Bogdanov, S.A., Vikharev, A.L., Luchinin, V.V., Golubkov, V.A., Ivanov, A.S., and Ilyin, V.A. **(2018)** "Emission properties of undoped and boron-doped nanocrystalline diamond films coated silicon carbide field emitter arrays", *JVST B*, 36, 021204.

Kuznetsova, M.A., Luchinin, V.V. **(2012)** "Focused Ion Beam Machining of SiC Field Emitters", *Nano and Microsystems Technology,* 12(149), 35-40 (in Russian, *Nano- i Mikrosistemnaya Tehnika*).

Young, R.D., and Mueller, E.W. **(1959)** "Experimental measurement of the total-energy distribution of field-emitted electrons", *Phys. Rev.,* 113, 115–120.

ACKNOWLEDGMENTS

The reported study was funded by RFBR, project number 20-07-01086

THANK YOU FOR YOUR ATTENTION!